ELSEVIER

Polymer 41 (2000) 8017–8026

polymer

www.elsevier.nl/locate/polymer

N-acetyl-4-nitro-1-naphthylamine as sensitizer of *N*,*N*-dimethylaniline for photoinitiated radical polymerization

A. Costela[a], I. García-Moreno[a,*], O. García[b], R. Sastre[b]

[a]*Instituto Química-Física "Rocasolano", Serrano 119, 28006 Madrid, Spain*
[b]*Instituto de Ciencia y Tecnología de Polímeros, Juan de la Cierva 3, 28006 Madrid, Spain*

Received 12 January 2000; received in revised form 14 February 2000; accepted 17 February 2000

Abstract

Photophysical, photochemical behaviour of *N*-acetyl-4-nitro-1-napthylamine (ANNA) in the presence of *N*,*N*-dimethylaniline (DMA) was analyzed to establish the influence of the nature of this nitroaromatic initiator on the photosensitized generation of free radicals during photoinitiated polymerization of lauryl acrylate (LA) monomer. Steady-state (365 nm) photolysis was studied providing experimental evidence of a photosensitization process of DMA through excitation energy transfer from ANNA. The dependence of the consumption rate of both reactants on the irradiation time reveals that up to 87 molecules of DMA are consumed for each ANNA molecule photoreduced in spite of the low photoreduction quantum yield of ANNA induced by DMA. The efficiency of the ANNA/DMA system as photoinitiator was studied by following the polymerization kinetics of LA monomer by Differential Scanning Photo-Calorimetry (Photo-DSC). The photosensitization of DMA, working concurrently to the photoreduction reaction, induces a polymerization efficiency up to 5 times higher than that reached with other nitroaromatic initiators.

Keywords: Photopolymerization; Nitroaromatic compounds; Photoinitiation

1. Introduction

Light-induced radical polymerization has been demostrated to have many applications, ranging from microelectronics to stereolithography [1–5]. As a consequence of the introduction of this process on an industrial scale, efforts are being made to provide better insights into the photophysical and photochemical processes involved, in order to develop new and more efficient photoinitiator molecules [6–10].

In a series of previous papers, the photoreactivity of *p*-nitroaniline (*p*NA) and its derivative, *p*-nitronaphthylaniline (NNA) as photoinitiators of polymerization in the presence of *N*,*N*-dimethylaniline (DMA) acting as reductor agent was analyzed [11–16]. The molecular structures of these derivatives are shown in Scheme 1 (Molecular structure of initiators *p*NA, NNA and ANNA and coinitiator DMA). These compounds were found to initiate the radical polymerization of lauryl acrylate (LA) monomer through a new and very efficient mechanism, involving the photosensitization of DMA by the initiator. This process, working concurrently with the photoreduction reaction, generates a cascade of free radicals derived from DMA without the consumption of initiator in a catalyzer-like way. As a result, the efficiency of polymerization was much higher than that obtained with well-known bimolecular photoinitiators of industrial importance, in spite of the new mechanism having a very low photoreduction quantum yield [15,16].

The new mechanism overturns the well-established photochemical behaviour on which the development of bimolecular photoinitiators has been based up to now. In the conventional approach, the generation of free radicals takes place through a stoichiometric photoreduction of the initiator induced, with a high quantum yield, by the coinitiator. In most of the well-known bimolecular photointiator systems, the reaction occurs from the triplet state of the initiator, formed with high yield under UV irradiation and characterized by a long lifetime (of the order of hundred of microseconds in solution at room temperature) which determines that the bimolecular photoreduction can compete efficiently with any other radiative or radiativeless decay channel [17]. In the new initiation mechanism, the triplet state of the initiator has to be a short-lived intermediate (of the order of a few nanoseconds or less), in order to enhance the efficiency of the excitation energy transfer with respect to other bimolecular deactivation reactions. Likewise, the triplet state of the coinitiator has to be very close in energy to the excited states

* Corresponding author. Tel.: +34-91-5619400; fax: +34-91-5642431.
E-mail address: iqrfm84@iqfr.csic.es (I. García-Moreno).

0032-3861/00/$ - see front matter
PII: S0032-3861(00)00170-1

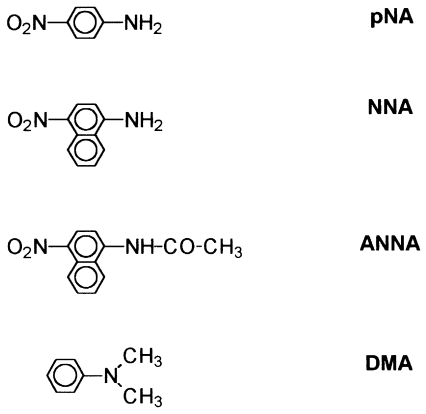

Scheme 1.

of the initiator and, in addition, the coinitiator molecule has to contain a bond with a dissociation energy lower than that of its triplet excited state, to induce its homolytic scission with formation of free radical initiating species.

In order to develop new photoinitiator systems fulfilling the energetic, photophysical and structural requirements aforementioned and to establish the actual possibilities and limitations of this new, promising mechanism of photosensitized polymerization, we have extended our study to a new derivative of *p*NA, namely *N*-acetyl-4-nitro-1-naphthylamine (ANNA) in the presence of DMA as bimolecular photoinitiator. The molecular structure of this new derivative is shown in Scheme 1. This disubstituted benzene has a proved efficiency as sensitizer in the photodimerization of cinnamoyl groups, which led to a previous study on its potential as photoinitiator of polymerization [18]. The present paper is devoted to relate the photophysical and photochemical behaviour of ANNA in the presence of DMA with its activity as photoinitiator of polymerization. To this aim, the stoichiometry of this bimolecular reaction was established by following the consumption rate of both reactants as a function of the irradiation time under steady-state photolysis conditions at 365 nm, at which wavelength ANNA absorbs strongly while DMA shows no significant absorption. Moreover, the dependence of the polymerization efficiency on both the oxygen presence and the molar ratio of DMA added to ANNA was analyzed following the polymerization of LA by Photo-DSC.

2. Method

2.1. Materials

Ethyl acetate (AcOEt) (Sigma-Aldrich, HPLC grade) was dried over molecular sieves with a pore diameter of 4 Å. *N*-acetyl-4-nitro-naphthylamine (ANNA) was obtained by direct reaction of 4-nitro-naphthylamine (4 g) with acetic anhydride (150 ml). The mixture was heated at about 100°C for 2 h and on cooling yellow crystals were formed, which were purified by subsequent recrystallizations from chloroform–ethanol mixtures. Its purity was checked by mass spectroscopy, NMR and UV. Lauryl acrylate (Fluka Chemie, Techn.) was distilled under reduced pressure prior to use. *N*,*N*-dimethylaniline (Carlo Erba) was dried over potassium hydroxide and then distilled under reduced pressure and stored under nitrogen atmosphere in the dark at low temperature.

2.2. Steady-state photolysis

The irradiation system and the experimental procedure employed have been described previously [11]. Briefly, the irradiation wavelength of 365 nm was selected from a Philips high-pressure mercury lamp (Hg-CS 500/2) with a Kratos monochromator (model GM 252). The absorbed light intensity at the irradiation wavelength was measured using an International Light digital radiometer (model IL 700). Aberchrome 540 actinometer [19] was used to calibrate the digital display of the radiometer to an absolute value for the number of quanta incident per unit of time. The photolysis of the sample was monitored by measuring the change in the maximum of the UV absorption curve.

2.3. Photocalorimetry

The kinetics of the polymerization was monitored using a Photo-DSC system [20]. ANNA was dissolved in pure LA at a concentration of $\approx 4 \times 10^{-3}$ M ensuring total absorption of the 365 nm wavelength radiation in the sample pan of 0.12 cm of path-length. The incident light intensity was kept constant at a value of 1.9×10^{-4} einstein l^{-1} s^{-1}. DMA was added as a coinitiator at concentrations ranging from 8×10^{-3} M to 1.2×10^{-1} M. Prior to irradiation, the sample of 20 μl was equilibrated into the calorimeter to the operating temperature at 40°C for 15 min. Then, the samples were irradiated for up to 15 min under aerobic and anaerobic conditions. A more detailed description of the general procedure followed and the determination of incident light intensity can be found elsewhere [20,21].

2.4. Measurement of the consumption rate of ANNA and DMA

The consumption rate of both components of this photoinitiating system was followed as a function of the irradiation time under steady-state photolysis conditions at 365 nm. The volume of the irradiated mixture in the quartz cell was 3.5 ml. At different irradiation times, aliquots of 25 μl were drawn from the medium to follow the conversion of DMA while the rest of the mixture was analyzed spectrophotometrically to follow the photoreduction of ANNA by measuring the decrease of its absorbance at the maximum wavelength (365 nm). The consumption of DMA was monitored by High Performance Liquid Chromatography (HPLC) (Waters M-45 HPLC pump, Spectra Physics 100 ultraviolet detector). The stationary phase was Spherisorb

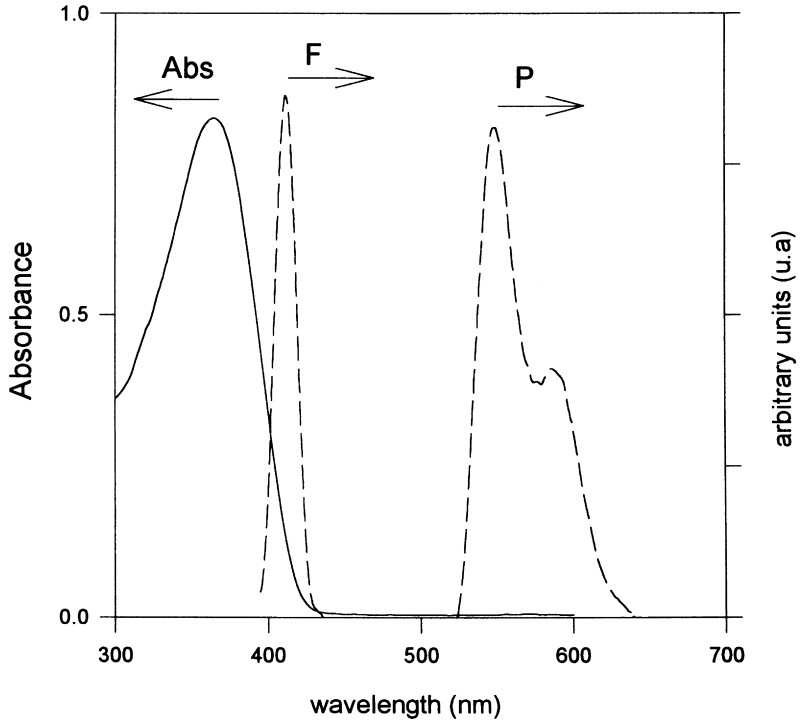

Fig. 1. Absorption (Abs), fluorescence (F) and phosphorescence (P) spectra (at 77 K) of a 1×10^{-4} M ethyl acetate solution of ANNA; excitation wavelength: 365 nm.

ODS-2-C_{18}, 5 μm (Trace Analytica) (125×4 mm^2 ID). The eluent was 7/3:methanol/water (v/v) + 1vol% of triethanolamine solution. The flow rate was 1 ml/min and the detector was set at 300 nm. DMA standards of 0.1–10 mM were run for a calibration curve. Under these conditions, the DMA retention time was 2.1 ± 0.1 min.

2.5. Spectroscopic measurements

The UV absorption spectra of the samples were recorded at room temperature with both Perkin–Elmer Lambda 16 and Shimadzu UV-265FS spectrophotometers. Emission spectra from the samples were recorded on a Perkin–Elmer LS-50B luminiscence spectrometer. Quantum yield of ANNA fluorescence (ϕ_f) was determined at room temperature by comparison with 9,10-diphenylanthracene as standard and assuming a value of 1 in cyclohexane [22]. Quantum yield of ANNA phosphorescence (ϕ_p) was obtained at 77 K by comparison with benzophenone as standard and assuming a value of 0.74 in ethanol [23].

3. Results and discussion

3.1. Spectroscopic characteristics

The absorption spectrum of ANNA in a 10^{-4} M ethyl acetate solution shown in Fig. 1 exhibits a broad band with its maximum being observed around 365 nm. The absorption maximum undergoes a pronounced shift to the blue from NNA (406 nm) to ANNA (365 nm) and *p*NA (356 nm). This hypsochromic shift is ascribed to a mutual electron withdrawing effect of the anilino nitrogens in ANNA and *p*NA molecules. This counteracts and eventually almost neutralizes the electron donating effect of the intervening aromatic group and results in the spectrum of ANNA being similar in both wavelength maximum and half-width to that of the unsubstituent *p*NA parent compound. The molar absorption coefficient of ANNA in ethyl acetate solution at 365 nm is 8261 M^{-1} cm^{-1}. The presence of a tertiary amine in the solution does not induce significant variations in the absorption characteristics of the initiator.

The emission spectra induced by irradiating at 365 nm a 10^{-4} M ethyl acetate solution of ANNA is also presented in Fig. 1. This acetyl derivative exhibits weak fluorescence ($\phi_f = 3.5 \times 10^{-5}$ centered at 411 nm) and phosphorescence emissions ($\phi_p = 1.8 \times 10^{-3}$), direct indication that an intersystem crossing between their excited states takes place in some extension. Phosphorescence spectrum, registered at 77 K with 0.1 ms time delay between excitation and detection, is centered at 530 nm with a triplet lifetime of 52 ms, much shorter than the pp^* triplet state of *p*NA (300 ms), revealing the np^* character of the lowest triplet state of ANNA molecule [24]. From the intercept point of the shortest wavelength of the phosphorescence emission curve with the abcise axis it could be deduced that the 0–0 position of this band to be at 509 nm.

Taking into account the spectroscopic characteristics of the coinitiator DMA, described in detail in a previous work

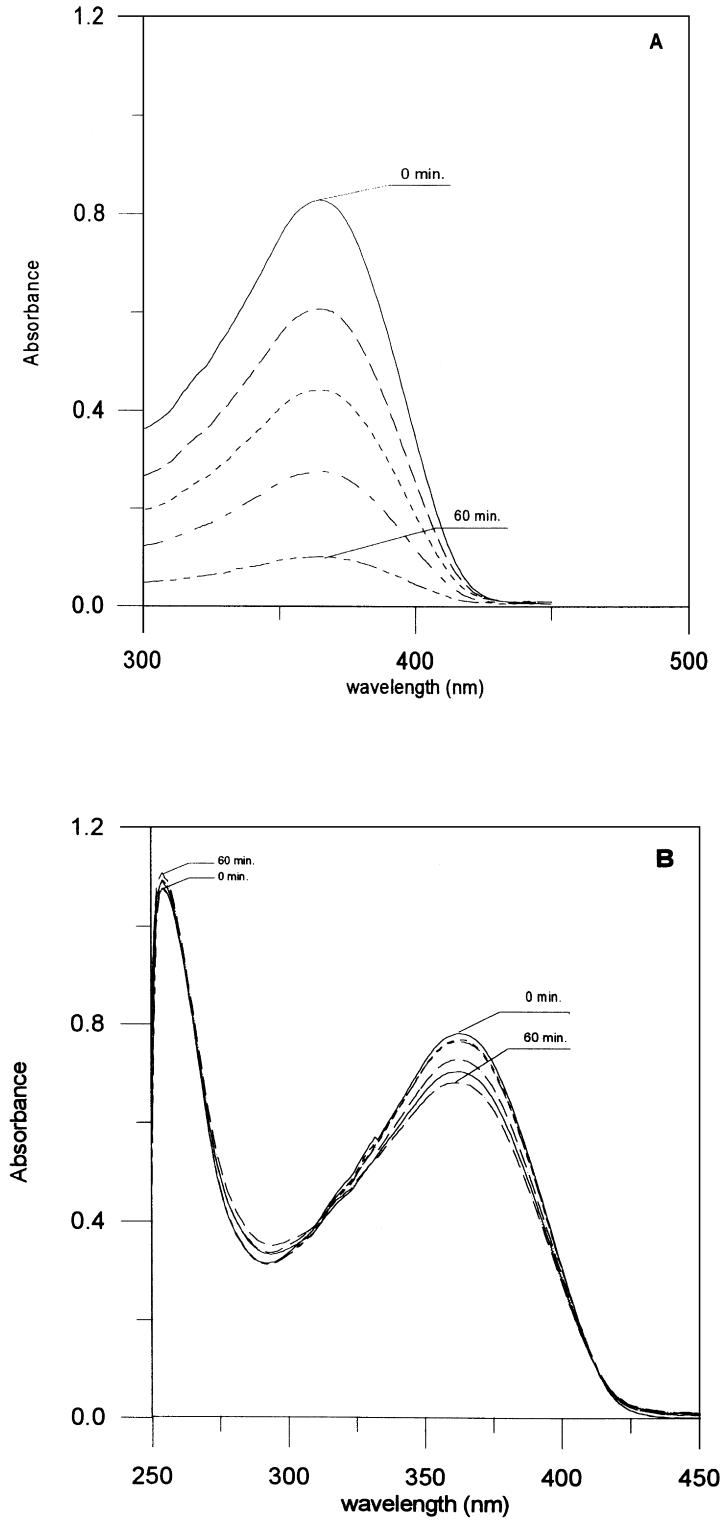

Fig. 2. Dependence of the UV–visible absorption spectrum of a 1×10^{-4} M ethyl acetate solution of ANNA on the irradiation time under steady-state conditions in both (A) anaerobic and (B) aerobic atmospheres; irradiation wavelength: 365 nm.

[16], it has be pointed out that the lowest-singlet state of ANNA is energetically very close to the lowest-triplet state of DMA. This energetic resonance could enhance the efficiency of the photosensitization process of DMA through excitation energy transfer from the excited ANNA.

3.2. Steady-state photolysis of ANNA

Steady-state photolysis of ANNA and its consumption rate, R_{ANNA}, were studied by irradiating a 10^{-4} M ethyl acetate solution of initiator at 365 nm under anaerobic

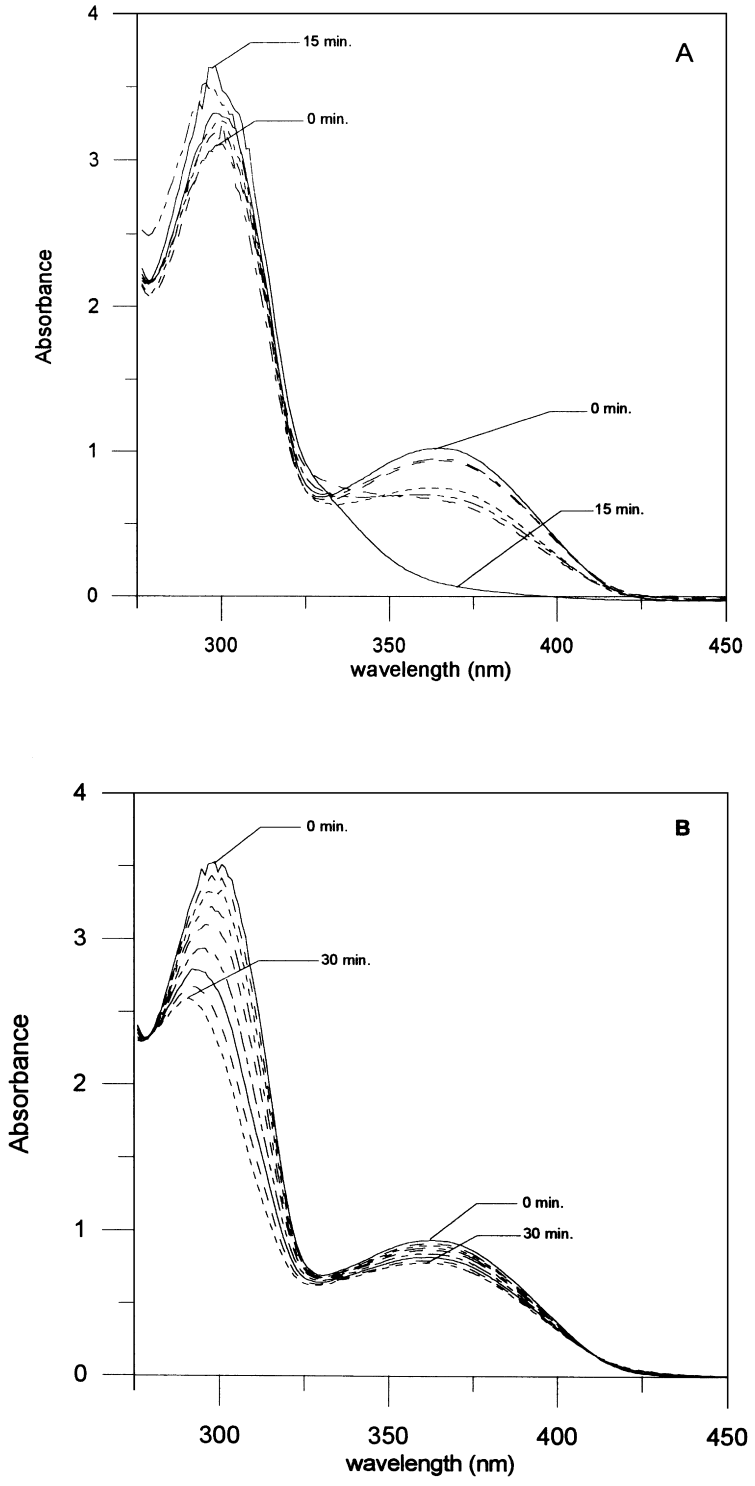

Fig. 3. Dependence of the UV–visible absorption spectrum of a 10^{-4} M ethyl acetate solution of ANNA with a molar ratio of DMA 1/10 on the irradiation time under steady-state conditions in both (A) anaerobic and (B) aerobic conditions; irradiation wavelength: 365 nm.

conditions with a constant incident light intensity, $I_0 = 5.1 \times 10^{-6}$ einstein l^{-1} s^{-1}. Quantum yields of chromophore disappearance, ϕ_{ANNA}, were determined by UV–visible spectroscopy following the decrease in the maximum of the initiator absorption band (365 nm) with the irradiation time as shown in Fig. 2. The steady-state photolysis of ANNA is characterized by a low quantum yield, $\phi_{ANNA} = 2.4 \times 10^{-3}$, reflecting its stability under UV irradiation. In addition, the disappearance of ANNA induced by irradiation under the above described experimental conditions, exhibits a linear dependence on the irradiation time, with its slope of 8.3×10^{-9} M s^{-1} being the consumption rate of ANNA,

Table 1
Influence (experimental conditions: photoinitiator concentrations, [ANNA] = 1×10^{-4} M; irradiation wavelength, $\lambda_{irr} = 365$ nm; incident light intensity, $I_0 = 1.4 \times 10^{-6}$ einstein l^{-1} s^{-1}) of the concentration of the coinitiator DMA on the photoreduction quantum yield of ANNA, ϕ_{ANNA}, and the consumption rate of both reactants, R_{ANNA} and R_{DMA}, under aerobic conditions, $[DMA]_r$ = initiator/DMA molar ratio

$[DMA]_r$	ANNA/DMA		
	$10^3\ \phi_{ANNA}$	$10^8\ R_{ANNA}$ (M s^{-1})	$10^8\ R_{DMA}$ (M s^{-1})
1/0	1.1	0.4	
1/2	3.3	0.2	21.0
1/5	6.0	0.7	47.0
1/10	8.3	1.0	49.3
1/20	8.5	1.0	54.6

R_{ANNA}. The *N*-acetylation does not have a significant effect on the photolysis process since the kinetic parameters of ANNA reach values similar to those determined for NNA derivative and slightly higher than that of *p*NA, all analyzed under identical experimental conditions [16].

In contrast to the behaviour exhibited by the two nitroaromatic initiators, *p*NA and NNA, the presence of oxygen reduces by a factor of 2 the rate and quantum yield of ANNA disappearance ($R_{ANNA} = 4.4 \times 10^{-9}$ M s^{-1}, $\phi_{ANNA} = 1.1 \times 10^{-3}$) in spite of the photolysis reaction occuring from a very short-lived triplet state. In addition, as can be seen in Fig. 2, the photolysis reaction of ANNA carried out under aerobic conditions leads to a slight increase with the irradiation time of the absorption intensity in the 275–300 nm spectral region. This behaviour could be related to the generation of photooxidation products able to absorb efficiently at similar wavelength than the initial ANNA derivative.

3.3. Photoreduction of ANNA by DMA

The photoreduction process of ANNA induced by DMA, studied under steady-state irradiation at 365 nm, for a 10^{-4} M initiator concentration and ANNA/DMA molar ratios of 1/2, 1/5, 1/10 and 1/20, was also followed by UV–visible spectroscopy. Fig. 3 shows the dependence on the irradiation time of the absorption spectrum of an ANNA/DMA 1/10 solution irradiated at 365 nm under both aerobic and anaerobic conditions. In a N_2 atmosphere, the chromophore disappearance, as revealed by the decrease in its absorption maximum, does not lead to a reduction of the absorption intensities at shorter wavelengths (300–325 nm) initially assigned to the tertiary amine. The analysis by HPLC reveals a rapid consumption of DMA under these experimental conditions. Thus, some photoreduction products have to absorb significantly in this spectral region and, consequently, increasing the absorption intensity of the band peaked at 310 nm during the photoreaction process. A different behaviour is observed when the photoreaction is carried out under aerobic conditions: the presence of oxygen decreases both the ANNA disappearance and the absorption

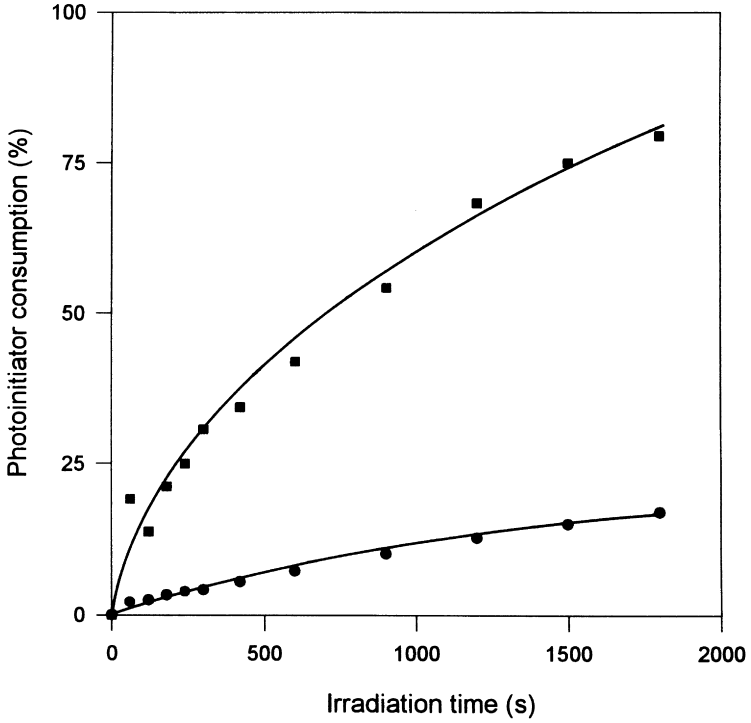

Fig. 4. Dependence of the consumption degree of ANNA (●) and DMA (■) on the steady-state irradiation time at 365 nm of a 10^{-4} M ethyl acetate solution of ANNA/DMA with a 1/10 molar ratio, under aerobic conditions, with an incident light intensity of $I_0 = 1.4 \times 10^{-6}$ einstein l^{-1} s^{-1}. The solid lines represent an eyeball fit to the data points.

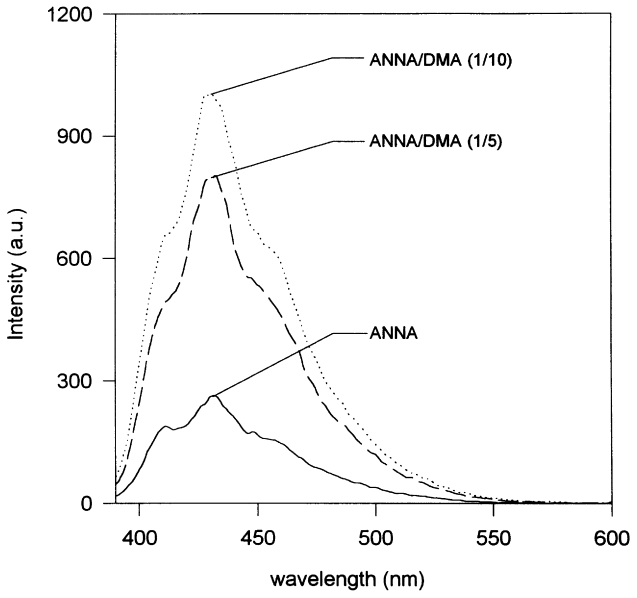

Fig. 5. Emission spectra of an ethyl acetate solution of ANNA with and without DMA after irradiation at 365 nm. The increasing (ANNA/DMA) molar proportions are indicated in parenthesis.

intensities at the shortest wavelengths revealing the consumption and photooxidation of DMA.

The photoreduction quantum yields of ANNA induced by DMA, ϕ_{ANNA}, under different experimental conditions, are summarized in Table 1. Following the same behaviour than that described for the *p*NA/DMA system [16], the presence of a tertiary amine as coinitiator induces an increase, up to a factor 7.6, of the chromophore disappearance quantum yield with respect to that determined in the photolysis process. By contrast to the *p*NA/DMA system, the parameter ϕ_{ANNA} increases with the molar proportion of DMA added to ANNA concentration.

As can be observed in Fig. 3, and following the same kinetic behaviour described previously for *p*NA and NNA [11,16], the parameter ϕ_{ANNA} results critically dependent on the presence of oxygen. Thus, under anaerobic conditions, the photoreduction quantum yield reaches a value up to 25 times higher than that determined in the presence of O_2. The lower efficiency of the photoreduction process under aerobic conditions could be ascribed to photooxidation reactions of the α-aminoalkyl radicals derived from the tertiary amine via a chain reaction competing effectively with ANNA photoreduction [25], as was discussed in a previous work [12]. At the same time, the photooxidation process leads to a decrease on the effective concentration of the coinitiator in the solution as is reflected in the drastic decrease of its absorption maximum at 290 nm with the irradiation time (see Fig. 3).

The consumption rate of ANNA and DMA, R_{ANNA} and R_{DMA}, respectively, were analyzed in a 10^{-4} M ethyl acetate solution of ANNA with different molar ratios to DMA irradiated, under aerobic conditions, at 365 nm with an incident light intensity $I_o = 1.4 \times 10^{-6}$ einstein l^{-1} s^{-1}. The values obtained for these kinetic parameters are summarized in Table 1.

Fig. 4 shows the dependence of the consumption of both reactants on the irradiation time. The DMA disappearance increases linearly and drastically with the irradiation time until a conversion degree near 50% is reached. Futher increases of the irradiation time beyond this point reduces the conversion rate of this tertiary amine. The consumption rates of DMA reported in Table 1 are deduced from the slope of the line fitted to these experimental data within the time interval where they exhibit a linear behaviour. For all ANNA/DMA molar ratios R_{DMA} is much higher than that of the photoinitiator and increases with the tertiary amine concentration although the relationship is not linear.

The consumption rate of DMA induced by ANNA is lower than that determined for *p*NA in spite of the lowest triplet state of DMA being energetically closer to the lowest excited singlet state of ANNA than that corresponding to *p*NA. The dependence of the consumption rate of DMA on the initiator could be ascribed to the influence of the nature and position of the substituent on the efficiency quantum yield of both the intersystem crossing and the fluorescence emission for each of these initiator molecules. These processes draw out molecules from the lowest excited singlet state of the initiator, reducing the extension and probability of the DMA photosensitization. Moreover, this dependence could also be related to a very high concentration of initiating radicals induced by ANNA which increases the probability of secondary reactions, specially second-order reactions such as primary radical recombinations that reduces consequently the apparent consumption of the coinitiator DMA.

The stoichiometry of the reaction, evaluated from the ratio of the slopes of the lines fitted to the consumption of both reactants, indicates that up to 87 molecules of DMA are consumed by each ANNA molecule photoreduced. Taking into account the low photoreduction quantum yield of ANNA promoted by DMA, the rapid conversion of the coinitiator confirms that the photoreduction process is competing with a photosensitization process of DMA through an excitation energy transfer from ANNA, yielding an avalanche of α-alkylamino radicals without the consumption of ANNA, following the effective mechanism described for photoinitiators such as *p*NA and NNA in the presence of DMA [9,12]. Experimental evidence of this photosensitization process is provided by the emission properties of an ethyl acetate solution of ANNA with and without DMA (Fig. 5). Irradiation at 365 nm of pure ANNA induces a weak emission centered at 411 nm, assigned to the fluorescence band of this derivative. The presence of DMA, which does not absorb at the irradiation wavelength, modifies the recorded emission increasing significantly its intensity. Taking into account that the DMA molecule emits phosphorescence in the same spectral region where fluorescence of ANNA appears with a quantum yield four orders of magnitude higher than ϕ_f of ANNA, the behaviour of the

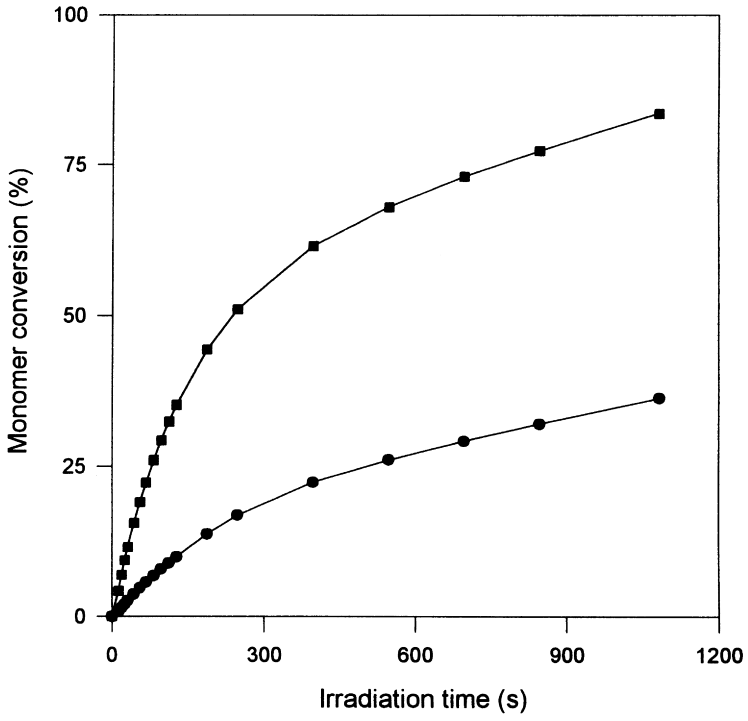

Fig. 6. Evolution of the conversion of LA monomer photoinduced by ANNA in the presence of a molar ratio to DMA of 1/2 with the irradiation time at 365 nm under aerobic (●) and anaerobic (■) conditions.

emission of the ANNA solution in the presence of increasing amounts of DMA is consistent with the phosphorescence of DMA being emitted concurrently with the fluorescence of ANNA. A more direct experimental evidence of the proposed process would require a time-resolved analysis in the subnanoseconds time domain due to the very short lifetimes involved.

3.4. Photoinitiation of polymerization

Different experiences have revealed that ANNA or DMA alone are unable of initiating polymerization of LA even over extensitive periods of time at 40°C in the dark or under illumination. When used in combination, however, they readily initiate LA polymerization but only under irradiation. This photoinitiated polymerization was found to be inhibited in the presence of hydroquinone, confirming that the process takes place by a radical mechanism. As was previously discussed for the *p*NA/DMA system, the radicals derived from the tertiary amine are the main and most active species in the initiation mechanism [14].

Table 2
Rate (R_p) and quantum yield (ϕ_m) of polymerization of LA photoinduced by the initiator ANNA in the presence of DMA as coinitiator, under aerobic and anaerobic conditions. $[DMA]_r$ = initiator/DMA molar ratio; steady-state concentration of oxygen in the sample $[O_2]_s$

$[DMA]_r$	$10^3 R_p$ (M s^{-1})		ϕ_m		$10^6 R_i$ (M s^{-1})		$10^8 [O_2]_s$ (M)
	N_2	O_2	N_2	O_2	N_2	O_2	
1/2	11.6	2.7	61.3	14.6	30.8	2.1	7.6
1/5	12.5	3.3	66.2	17.5	35.7	2.2	7.2
1/10	12.8	3.7	67.7	19.7	37.3	3.2	6.6
1/20	11.7	3.7	61.8	19.4	31.1	3.1	5.5
1/30	11.1	3.8	58.5	20.2	28.2	3.3	4.7

The kinetic of photoinitiation of LA was monitored by Photo-DSC. Exotherm rates as a function of time were observed under isothermal conditions for continuous illumination reactions. Initial rates of polymerization R_p were calculated from the slopes of the plots of polymerized monomer concentration versus irradiation time, in the time interval where this conversion change exhibits a linear behavior (see Fig. 6). Polymerization quantum yields (ϕ_m) were determined from the slope of the line best fitting the experimental linear dependence found when the amount of monomer polymerized is represented as a function of the absorbed light intensity, I_a.

The rate of initiation, R_i, was calculated from the general expression for the steady-state free radical photoinitiated polymerization:

$$R_p = \frac{k_p}{k_t^{1/2}}[M]R_i^{1/2}$$

where [M] is the monomer concentration, k_p and k_t are the rate constants of propagation and termination, respectively, which for the acrylate monomers are typically of the order of $\approx 10^3$ and $\approx 3 \times 10^6$ M^{-1} s^{-1}, respectively [26].

The influence of DMA concentration on the polymerization process is reflected in Table 2. The values of all parameters increase with amine concentration, reaching a

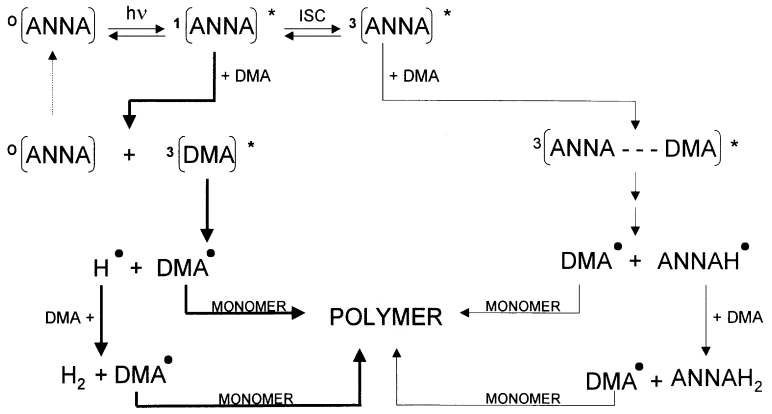

Fig. 7. Mechanism for the photoreaction of ANNA in the presence of DMA under UV irradiation. The photoreduction process (right) is a minor pathway as compared with the efficient photosensitization process of DMA by ANNA (left) leading to an enhanced polymerization activity in spite of a very low photoreduction quantum yield.

maximum for the ANNA/DMA molar ratio of 1/10. Further increases in the DMA concentration induce slight decreases in the values of all the parameters. The observed behaviour could be explained by taking into account that the probability of generating exciplex ANNA/DMA and, consequently, initiator radicals increases with the amine concentration up to a point.

Under aerobic conditions the kinetic parameters of photopolymerization are, at least, three times lower than those determined in nitrogen atmosphere (see Table 2). This effect reveals the role of molecular oxygen as inhibitor of radical-induced polymerization because of its high reactivity toward radical species. Taking into account that the photooxidation rate constant is 10^5 times greater than that of polymerization propagation, the initiator radicals will react predominantly with oxygen and the polymerization would only take place when the oxygen concentration drops to levels low enough for the monomer to be able to compete with the oxygen molecules in the reaction with the initiator radicals. In our system, no inhibition period was detected in the aerobic polymerization process, in spite of the photooxidation reactions of the radicals discussed above. In an open air system, such as the present one, a stationary concentration of dissolved oxygen is reached as a balance between oxygen consumption in the sample and oxygen diffusion from the atmosphere. Moreover, the presence of a tertiary amine (DMA), which is known to consume oxygen by a chain process [25], produces a fast decay of the oxygen concentration, shortening the duration of the inhibition period to a value below the temporal resolution (0.1 s) of the calorimetric technique used in this work to characterize the polymerization kinetics.

The steady-state concentration of oxygen, $[O_2]_s$, can be calculated from the equation proposed by Decker and Jenkins [27]:

$$[O_2]_s = \frac{(R_i k_t)^{1/2}}{k_0}\left\{\frac{(R_p)_{N_2}}{(R_p)_{O_2}} - \frac{(R_p)_{O_2}}{(R_p)_{N_2}}\right\}$$

where k_0 is the rate constant of radical scavenging by O_2 ($\approx 5\times10^8\ M^{-1}\ s^{-1}$) and $(R_p)_{O2}$ and $(R_p)_{N2}$ are the rates of polymerization with and without oxygen, respectively.

The stationary concentrations of oxygen calculated from this equation are reported in Table 2. As was expected, this parameter decreases as the DMA concentration increases. The obtained results imply that, under the given experimental conditions, the concentration of oxygen dissolved in the system ($\approx 10^{-3}$ M) has to drop by five orders of magnitude to reach its stationary level at the beginning of the polymerization. According to the above discussion, this reduction of the oxygen concentration should happen in less than 0.1 s.

The polymerization rate and efficiency induced by ANNA/DMA reveal an initiator system more efficient in the polymerization process than in the photoreduction reaction, a direct consequence to the generation up to 87 α-alkylamino radicals from DMA for each ANNA molecule photoreduced. In addition, it has to be remarked that, although the consumption rate of DMA induced by ANNA is lower than that determined by *p*NA, the acetylation of the naphthyl derivative ANNA results in a remarked increase of its polymerization activity with respect to that exhibited by *p*NA, specially for initiator/DMA molar ratios ranging from 1/2 to 1/10 [16].

The enhanced polymerization activity reached with the ANNA/DMA system could be a direct consequence of a higher efficiency in the photosensitization process of the triplet state of DMA by ANNA. This process yields an avalanche of α-alkylamino radicals derived from DMA which, in the presence of the acrylate monomer with the molar concentration selected to carry out a bulk polymerization, increases significantly the rate and effectiveness of the initiation process, reducing the extension and probability of other secondary reactions with concentrations of reactives much lower than that of the monomer. Taking into account that the stoichiometry analysis was analyzed in the absence of monomer, the aforementioned differences observed between the kinetic behaviour of the

photoreduction process and the polymerization reaction could explain why this initiator system exhibits a higher polymerization efficiency with a lower R_{DMA}. In order to confirm this conclusion, an in situ and real-time analysis of the radical generation would be required. Work along this line is in progress.

The results and conclusions obtained in the present study, together with those obtained in the analysis of other photoinitiator systems based on nitroaromatic compounds [13,15,16], strongly suggest the pathways indicated in Fig. 7 as the most probable mechanism for the photoreaction of ANNA in the presence of DMA under UV irradiation. The photosensitization process of the triplet state of DMA by ANNA is reflected in an enhancement of the polymerization efficiency with respect to other conventional bimolecular photoinitiators, such as aromatic ketones benzophenone and Michler's ketone [12]. In addition, the ANNA/DMA initiating system induces a polymerization efficiency up to 5 times higher than that reached with other nitroaromatic derivatives, based on *p*NA/DMA and NNA/DMA, where the same proposed mechanism of photosensitized reaction is followed [15,16]. This increase in polymerization efficiency could be due to the fact that the triplet state of DMA is nearly resonant to the first excited singlet state of ANNA, which reduces, with respect to *p*NA and NNA initiators, the energetic differences between the states involved in the excitation energy transfer and increases significantly the extension and effectiveness of the photosensitization process. A direct consequence of this closer resonance is an increase in the polymerization efficiency which confirms the good performance of this new and promising mechanism of polymerization. Moreover, and taking into account that the initiator ANNA is the active species in the absorption of the irradiation light, the low consumption of ANNA during the photoreduction process is also assuring a high efficiency of the primary step of this initiating mechanism. The high-initiation efficiency achieved with a reduced consumption of the initiator represents a significant economical advantage from an industrial point of view.

Acknowledgements

This work was supported by the Projects MAT97-0705-C02-01 and MAT97-0727 of the Spanish CICYT.

References

[1] Brickman E, Delzenne G, Poot A, Willems J. Unconventional imaging processes. Focal Press, 1977.
[2] Pappas SP. UV curing: science and technology, vol. 1. Stanford Technology Marketing Corporation, 1978.
[3] Pappas SP. UV curing: science and technology, vol. 2. Stanford Technology Marketing Corporation, 1982.
[4] Roffey GC. Photopolymerization of surface coatings. Chichester, UK: Wiley-Interscience, 1982.
[5] Phillips R. Sources and applications of ultraviolet radiation. New York: Academic Press, 1983.
[6] Roffey CG. Photogeneration of reactive species for UV curing. Chichester: Wiley, 1997.
[7] Fouassier JP. In: Rabek JF, editor. Photochemistry and photophysics, vol. II. Boca Raton, FL: CRC Press, 1990 (chap. 1).
[8] Lissi EA, Encinas MV. In: Rabek JF, editor. Photochemistry and photophysics, vol. IV. Boca Raton, FL: CRC Press, 1991 (chap. 4).
[9] Dietliker KK. In: Oldring PKT, editor. Chemistry and technology of UV and EB formulations for coating, inks and paints, vol. 3. London: Sita Technology, 1991.
[10] Fouassier JP, Rabek JF, editors. Radiation curing in polymer science and technology, vol. IV. London: Elsevier, 1993.
[11] Costela A, García-Moreno I, Dabrio J, Sastre R. J Photochem Photobiol A: Chem 1997;109:77.
[12] Costela A, García-Moreno I, Dabrio J, Sastre R. J Polym Sci A: Polym Chem 1997;35:3801.
[13] Costela A, García-Moreno I, Dabrio J, Sastre R. Acta Polym 1997;48:423.
[14] Costela A, García-Moreno I, Dabrio J, Sastre R. Macromol Chem Phys 1997;198:3787.
[15] Costela A, García-Moreno I, García O, Sastre R. Chem Phys Lett 2000 (in press).
[16] Costela A, García-Moreno I, García O, Sastre R. J Photochem Photobiol A: Chem 2000;131:133.
[17] Costela A, Dabrio J, Figuera JM, García-Moreno I, Gsponer H, Sastre R. J Photochem Photobiol A: Chem 1995;92:213.
[18] Sastre R, Conde M, Mateo JL. J Photochem Photobiol A: Chem 1988;44:111.
[19] Heller HG, Langan JR. J Chem Soc Perkin Trans 1981;2:341.
[20] Sastre R, Conde M, Catalina F, Mateo JL. Rev Plas Mod 1989;393:375.
[21] Mateo JL, Bosch P, Catalina F, Sastre R. J Polym Sci Polym Chem Ed 1992;30:829.
[22] Scaiano JC. Handbook of organic photochemistry. Boca Raton, FL: CRC Press, 1989 (chap. 16).
[23] Demas JN, Grasby GA. J Phys Chem 1971;75:91.
[24] Malkin J. Photophysical and photochemical properties of aromatic compounds. Boca Raton, FL: CRC Press, 1992 (chap. 14).
[25] Bartholomew RF, Davidson RS. J Chem Soc C 1971:2342.
[26] Liaw DJ, Chung KC. J Chin Inst Chem Engng 1982;13:145.
[27] Decker C, Jenkins AD. Macromolecules 1985;18:1241.